



Deposited via The University of Sheffield.

White Rose Research Online URL for this paper:

<https://eprints.whiterose.ac.uk/id/eprint/175859/>

Version: Published Version

---

**Article:**

Sun, W., Taylor, C.S., Zhang, Y. et al. (2021) Cell guidance on peptide micropatterned silk fibroin scaffolds. *Journal of Colloid and Interface Science*, 603. pp. 380-390. ISSN: 0021-9797

<https://doi.org/10.1016/j.jcis.2021.06.086>

---

**Reuse**

This article is distributed under the terms of the Creative Commons Attribution (CC BY) licence. This licence allows you to distribute, remix, tweak, and build upon the work, even commercially, as long as you credit the authors for the original work. More information and the full terms of the licence here:

<https://creativecommons.org/licenses/>

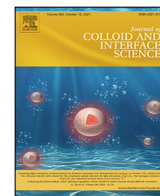
**Takedown**

If you consider content in White Rose Research Online to be in breach of UK law, please notify us by emailing [eprints@whiterose.ac.uk](mailto:eprints@whiterose.ac.uk) including the URL of the record and the reason for the withdrawal request.



Contents lists available at ScienceDirect

## Journal of Colloid and Interface Science

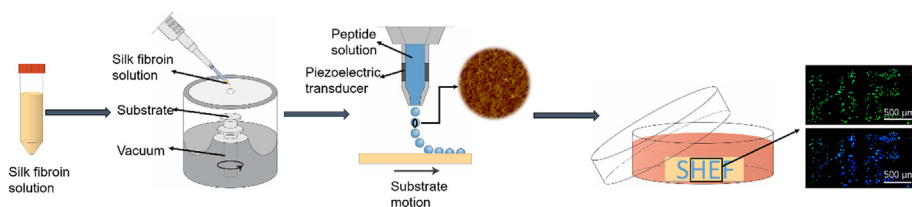
journal homepage: [www.elsevier.com/locate/jcis](http://www.elsevier.com/locate/jcis)

## Regular Article

## Cell guidance on peptide micropatterned silk fibroin scaffolds

Weizhen Sun<sup>a</sup>, Caroline S. Taylor<sup>b</sup>, Yi Zhang<sup>a</sup>, David A. Gregory<sup>a,b</sup>, Mhd Anas Tomeh<sup>a</sup>, John W. Haycock<sup>b</sup>, Patrick J. Smith<sup>c</sup>, Feng Wang<sup>d</sup>, Qingyou Xia<sup>d</sup>, Xiubo Zhao<sup>a,e,\*</sup><sup>a</sup> Department of Chemical and Biological Engineering, University of Sheffield, Sheffield S1 3JD, UK<sup>b</sup> Department of Materials Science & Engineering, University of Sheffield, Sheffield S1 3JD, UK<sup>c</sup> Department of Mechanical Engineering, University of Sheffield, Sheffield S1 4BJ, UK<sup>d</sup> Biological Science Research Centre, Chongqing Key Laboratory of Sericultural Science, Chongqing Engineering and Technology Research Centre for Novel Silk Materials, Southwest University, Chongqing 400715, China<sup>e</sup> School of Pharmacy, Changzhou University, Changzhou 213164, China

## GRAPHICAL ABSTRACT



## ARTICLE INFO

## Article history:

Received 12 February 2021

Revised 27 May 2021

Accepted 14 June 2021

Available online 17 June 2021

## Keywords:

Nerve tissue engineering

Micro-patterning

Inkjet printing

Self-assembling peptides

PC12 cells

## ABSTRACT

Guiding neuronal cell growth is desirable for neural tissue engineering but is very challenging. In this work, a self-assembling ultra-short surfactant-like peptide I<sub>3</sub>K which possesses positively charged lysine head groups, and hydrophobic isoleucine tails, was chosen to investigate its potential for guiding neuronal cell growth. The peptides were able to self-assemble into nanofibrous structures and interact strongly with silk fibroin (SF) scaffolds, providing a niche for neural cell attachment and proliferation. SF is an excellent biomaterial for tissue engineering. However neuronal cells, such as rat PC12 cells, showed poor attachment on pure regenerated SF (RSF) scaffold surfaces. Patterning of I<sub>3</sub>K peptide nanofibers on RSF surfaces significantly improved cellular attachment, cellular density, as well as morphology of PC12 cells. The live / dead assay confirmed that RSF and I<sub>3</sub>K have negligible cytotoxicity against PC12 cells. Atomic force microscopy (AFM) was used to image the topography and neurite formation of PC12 cells, where results revealed that self-assembled I<sub>3</sub>K nanofibers can support the formation of PC12 cell neurites. Immunolabelling also demonstrated that coating of I<sub>3</sub>K nanofibers onto the RSF surfaces not only increased the percentage of cells bearing neurites but also increased the average maximum neurite length. Therefore, the peptide I<sub>3</sub>K could be used as an alternative to poly-L-lysine for cell culture and tissue engineering applications. As micro-patterning of neural cells to guide neurite growth is important for developing nerve tissue engineering scaffolds, inkjet printing was used to pattern self-assembled I<sub>3</sub>K peptide nanofibers on RSF surfaces for directional control of PC12 cell growth. The results demonstrated that inkjet-printed peptide micro-patterns can effectively guide the cell alignment and organization on RSF scaffold surfaces, providing great potential for nerve regeneration applications.

© 2021 The Author(s). Published by Elsevier Inc. This is an open access article under the CC BY license (<http://creativecommons.org/licenses/by/4.0/>).

\* Corresponding author.

E-mail address: [xiubo.zhao@sheffield.ac.uk](mailto:xiubo.zhao@sheffield.ac.uk) (X. Zhao).

## 1. Introduction

The human nervous system is composed of the central nervous system (CNS) and the peripheral nervous system (PNS), which can be easily impaired by injuries, such as trauma and car accidents, as well as diseases, including Alzheimer's disease, Parkinson's disease, strokes and brain tumours.[1–3] Regeneration of both damaged CNS and PNS is challenging in tissue engineering.[3–5] It is therefore vitally important to develop well-defined functional scaffolds for nerve tissue regeneration to help guide neural cell attachment, alignment, spreading and proliferation.[6–8]

In addition, alignment and interconnection of neuronal cells *in vitro* allows the mimicking of neuronal architectures *in vivo* and help in understanding the underlying mechanisms needed to promote and accelerate regeneration of damaged neural tissue. Micro-patterning technology, which has already attracted significant attention, can enable the geometric control of neuronal cell alignment.[9–12] Lithography, including ultraviolet lithography (UVL), soft lithography (SL) and electron-beam lithography (EBL), is a traditional technology for micro-patterning proteins onto substrates.[13,14] Compared to UVL and EBL, SL is a convenient technique,[15] which has been widely used to micro-pattern neuronal cells.[9,10,12] For example, micro-patterned polydimethylsiloxane (PDMS) has been shown to enhance the attachment, alignment, spreading, proliferation, neurite formation and elongation of neuronal cells.[12] However, SL needs to be operated in a high-standard clean room, and samples can be easily contaminated during fabrication.[16,17] Inkjet printing, on the other hand, is a cost-effective and flexible micro-patterning technique which is capable of patterning complex geometries at high precision.[13,14] Moreover, as inkjet printing is a non-contact technique, cross-contamination of the final product is significantly reduced. Therefore, it was used as a micro-patterning technique to pattern self-assembled peptide nanofibers on regenerated silk fibroin (RSF) surface to guide the growth of neuronal PC12 cells in this study.

Silk fibroin (SF), extracted from *Bombyx mori* (*B. mori*), has received significant attention due to its biocompatibility, tuneable biodegradability, low immunogenicity and excellent mechanical properties.[18,19] RSF possesses tuneable rheological properties and can be used to fabricate different types of scaffolds, such as hydrogels,[20] films[21] and sponges.[22] These scaffolds have been successfully applied in a variety of tissue engineering applications, such as skin,[23] vascular[24] and musculoskeletal tissue engineering to match the different properties of autologous tissues.[25] However, *B. mori* silk lacks the cell adhesive components, such as arginine-glycine-aspartic acid (RGD) sequence, which promotes cell attachment.[26–28] Therefore, without the addition of cell adhesive molecules, such as poly-L-lysine (PLL), and extracellular matrix (ECM) components, silk scaffolds normally have poor cell attachment,[29,30] which is particularly significant for neuronal cells.[31]

Cell adhesive molecules have been successfully applied as scaffolding materials in nerve tissue engineering.[32] During the last two decades, peptide sequences such as RGD, YIGSR and IKVAV have been used to promote neuronal cell attachment, proliferation, and neurite outgrowth.[33,34] Self-assembled peptide nanofibers (such as RADA16, EAK16) are novel biomaterials that can be fabricated through bottom-up approach and have the potential to be used as scaffold materials for tissue engineering.[35,36] Surfactant-like peptide AC-I<sub>3</sub>K-NH<sub>2</sub> (I<sub>3</sub>K) has an acetyl group on its N terminal and its C terminal was blocked by an amine group. Three hydrophobic isoleucine (Ile or I) and one hydrophilic lysine residue (Lys or K) causes the peptide to possess the surfactant feature and promote the self-assembly of I<sub>3</sub>K into long and uniform nanofibers in aqueous solutions with the K residues on the outside

of the nanofibers.[37,38] Positively charged PLL has been shown to promote neuronal cell attachment.[39] Therefore, it is anticipated that the self-assembled I<sub>3</sub>K peptide nanofibers also have great potential as a cell adhesive matrix for nerve tissue regeneration.

In this study, RSF/I<sub>3</sub>K peptide scaffolds were fabricated to guide neuronal cell attachment. The coating and patterning of peptide nanofibers were achieved through spin coating and inkjet printing, respectively. The glass/silicon wafer substrates were coated with a layer of negatively charged RSF[40] before the coating, or printing, of peptide nanofiber solutions. The cationic peptide nanofibers adhered onto the RSF surfaces through charge-charge interactions. Rat pheochromocytoma (PC12) cells were cultured onto RSF/I<sub>3</sub>K scaffolds to investigate the effect of the I<sub>3</sub>K peptide nanofibers on cell attachment, proliferation and viability. Atomic force microscopy (AFM) was used to further analyse cell morphology, height and footprint on the RSF/I<sub>3</sub>K scaffold surfaces.[41] The results indicated that I<sub>3</sub>K peptide nanofibers promoted cell attachment, proliferation and neurite outgrowth of PC12 cells. Immunolabelling also demonstrated that coating of I<sub>3</sub>K nanofibers onto RSF surfaces, not only increased the percentage of cells bearing neurites, but also increased the average maximum neurite length. Cells attached along the inkjet-printed peptide nanofiber patterns, demonstrating that inkjet printing is a promising technique to pattern scaffolds for geometrical guidance of neuronal cell growth as well as investigation of neurite development and formation *in vitro*.[42]

## 2. Experimental section

### 2.1. Materials

The peptide Ac-I<sub>3</sub>K-NH<sub>2</sub> (purity > 98%, w/w) was purchased from GL Biochem Ltd. (Shanghai, China). *B. mori* silkworm cocoons were supplied by Biological Science Research Centre, Southwest University, China. PC12 Adh (CRL-1721.1) cell line was obtained from the American Type Culture Collection (ATCC). Silicon wafers were purchased from Compact Technology Ltd, UK. Unless otherwise specified, chemicals and reagents (analytical grades) were purchased from Sigma Aldrich, UK.

### 2.2. Preparation of regenerated silk fibroin

*B. mori* silkworm cocoons were cut into small pieces (~1 cm<sup>2</sup>) and degummed in 0.02 M Na<sub>2</sub>CO<sub>3</sub> solution at 100 °C for 1.5 h under stirring. Degummed silk was rinsed three times with deionized water (DI water) to ensure the removal of sericin. After which the degummed silk fibres were dried for 2 days in a drying oven at 60 °C and dissolved under stirring in Ajisawa's reagent (CaCl<sub>2</sub>/ethanol/deionized water = 1:2:8 M ratio) at 80 °C for 1.5 h. The resulting viscous solution was dialyzed against DI water until a conductivity below 10 μS of the dialysis fluid was reached. The resulting RSF solution was then centrifuged for 10 min at 10,000 rpm to remove any particulates. The RSF concentration was determined by weighing dried RSF peptide residues on microscope slides. Stock RSF solutions of 5 mg/mL and 40 mg/mL were made by diluting with DI water and stored at 4 °C prior to use.

### 2.3. Preparation of RSF / peptide samples

I<sub>3</sub>K peptides were dissolved in 20 mM HEPES buffer (pH 6.0) at 5 mg/mL and incubated for 7 days under ambient conditions for self-assembly. The sample was then diluted with 20 mM HEPES buffer (pH 6.0) to 4, 3, 2, 1 mg/mL prior to use. RSF/peptide bilayer scaffolds were made by spin coating (Laurell Technologies Corporation, USA) onto 1 cm<sup>2</sup> microscope cover glasses or silicon wafers. The first layer of RSF (30 μL, 8,000 rpm, 25 s) was coated followed

by fixing using 95% wt/vol ethanol (20  $\mu$ L, 4,000 rpm, 25 s), to convert the RSF layer from soluble random coil structure (silk I) to insoluble  $\beta$ -sheet structure (silk II).[43] The second layer, i.e. the positively charged peptide (30  $\mu$ L, 8,000 rpm, 25 s) was coated and adhered onto the negatively charged RSF substrate via charge interaction. The solution concentration ratios of RSF/peptide were 5:0; 40:0; 40:1; 40:2; 40:3; 40:4; 40:5 and 0:5, respectively.

#### 2.4. Atomic force microscopy

AFM measurement (Bruker Dimension Icon, Bruker Corporation, USA) was performed in tapping model with SCANASYST-AIR probes at room temperature. To image peptide nanostructures, peptide solution was dropped onto freshly cleaved mica and dried under gentle air flow. AFM was also used to characterise the topography of the RSF/I<sub>3</sub>K scaffolds and attached cells. PC12 neuronal cells were fixed with 3.7% paraformaldehyde (PFA) in phosphate buffered saline (PBS) for 45 min at room temperature. The PBS solution was then removed carefully with a pipette and the samples were washed with DI water gently to avoid crystallisation of PBS buffer salts. The samples were then left to dry at room temperature for 1 min prior to AFM characterisation. Images were analysed by NanoScope Analysis software (Version 1.5).

#### 2.5. Inkjet printing

All glass slide surfaces were cleaned with 5% Decon90 solution and rinsed with plenty of DI water before printing: 1 layer of RSF solution (40 mg/mL) was coated via spin coating on the glass slides (30  $\mu$ L per  $\text{cm}^2$ , 8000 rpm, 25 s) followed by 95% wt/vol ethanol solution (20  $\mu$ L, 4000 rpm, 25 s) via spin coating. A Jetlab 4xL (MicroFab Inc., Texas, US) equipped with a piezoelectric drop-on-demand (DoD) jetting device (60  $\mu$ m nozzle diameter) was used for the printing of the I<sub>3</sub>K peptide nanofiber ink. The actuation voltage and frequency used were 90 V and 300 Hz, respectively. The distance between the nozzle tip and the substrate was approximately 10 mm. To investigate the effect of printed I<sub>3</sub>K peptide nanofiber pattern on the growth of PC12 cells, 1 layer of the pattern "SHEF" was printed.

#### 2.6. Culture of PC12 neuronal cells on scaffolds

PC12 neuronal cells were cultured in Dulbecco's Modified Eagle Medium (DMEM) with high glucose and supplemented with 10% foetal calf serum (FCS), 1% penicillin/streptomycin, 1% glutamine and 0.5% fungizone in an incubator at 37 °C under 5% (v/v) CO<sub>2</sub>. The medium was replaced every 3 days. RSF/I<sub>3</sub>K scaffolds were sterilized under ultraviolet light for 30 min before being washed in PBS for three times, and then placed in 12 well plates under metal rings (to secure the samples). Confluent cells were detached with 0.25% (w/v) trypsin-EDTA (ethylenediaminetetraacetic acid) and then seeded onto scaffolds' surface at 10,000 cells/ $\text{cm}^2$  through the holes of metal rings. These samples were cultured in DMEM medium containing 10% FCS for 6 days.

#### 2.7. Cell adhesion assay

Following incubation, neuronal cells were fixed in 3.7% PFA for 45 min at room temperature followed by washing twice with PBS and incubated for a further 45 min with 0.1% Triton X-100. Finally, the cells were washed twice with PBS and stained with FITC-phalloidin to visualize actin filaments and 4,6-diamidino-2-phenylindole dihydrochloride (DAPI) to visualize the nuclei. The samples were then imaged using a fluorescence microscope (Nikon Eclipse LV100).

#### 2.8. Resazurin assay

Metabolic activity of PC12 cells was assessed after 24, 72, and 144 h in culture. Culture medium was removed, and samples were cultured in a 100  $\mu$ M resazurin salt in PBS, and assay dependent culture media for 4 h at 37 °C and 5% CO<sub>2</sub>. Triplicates of 100  $\mu$ L of reduced formazan product, were then transferred to a black 96 well plate and the fluorescence was read in a FLx800 fluorescence plate reader (Biotek Instruments Inc.) at 540/635 nm. Background fluorescence readings were measured and subtracted from results.

#### 2.9. Live and dead assay

A live / dead assay was carried out by exchanging the medium with serum-free medium containing 0.001% (v/v) Syto-9™ (Invitrogen) and 0.0015% (v/v) propidium iodide (PI) and then incubated for 30 min in an incubator at 37 °C under 5% (v/v) CO<sub>2</sub>. The samples were then imaged using an upright Zeiss LSM 510 confocal microscope. An argon ion laser was used to visualise live cells stained with Syto-9™ ( $\lambda_{\text{ex}} = 494 \text{ nm}$  /  $\lambda_{\text{em}} = 515 \text{ nm}$ ) and a helium–neon laser for dead cells stained with PI ( $\lambda_{\text{ex}} = 536 \text{ nm}$  /  $\lambda_{\text{em}} = 617 \text{ nm}$ ). ImageJ software (National Institutes of Health, USA) was used to count the number of live and dead cells for several images of 2500  $\mu\text{m}^2$  sample areas randomly and averaged. Microscope images were converted to grayscale 8-bit images and then converted to a binary image via selecting the best threshold to generate a high contrast image, cell number was then counted via the 'analyse particles' algorithm in ImageJ.

#### 2.10. Immunostaining of the neurites assay

Neuronal cell differentiation, on samples, was assessed by measuring the lengths of neurites extending from cells. PC12 cells were washed with PBS before cells were fixed with 3.7% (v/v) PFA for 20 min at room temperature. Following a PBS wash, cells were permeabilized with 0.1% Triton X-100 for 20 min, at room temperature and unreactive binding sites were blocked with 3% bovine serum albumin (BSA) in PBS for 30 min. PC12 cells were incubated with a mouse anti- $\beta$  III-tubulin (neurite marker) antibody (1:250 dilution from Promega, Chilworth, United Kingdom) diluted in 1% BSA in PBS and incubated at 4 °C for 24 h. After a PBS wash, PC12 cells were labelled with Texas Red-conjugated anti-mouse IgG antibody (1:200 dilution in 1% BSA from Vector Labs, Burlingame, USA) in 1% BSA, for 90 min at room temperature. Samples were imaged with an upright Zeiss LSM 510 confocal microscope, using a helium–neon laser (543 nm) for Texas Red excitation ( $\lambda_{\text{ex}} = 589 \text{ nm}$  /  $\lambda_{\text{em}} = 615 \text{ nm}$ ). Images were analysed, and neurites were measured using the ruler tool on ImageJ software.

#### 2.11. Statistical analysis

GraphPad Prism V.6 software was used to analyse data quantitatively. One-way or two-way analysis of variance (ANOVA) with multiple comparisons was used for all multiple group experiments, and equality of variances was confirmed by Tukey's multiple comparisons test. P values < 0.05 were deemed significant. Values in graphs are presented as mean  $\pm$  one standard deviation.

### 3. Results and discussion

#### 3.1. Attachment of PC12 neuronal cells on SF films

RSF scaffolds have been extensively used in tissue engineering applications.[23] However, pure RSF lacks cell recognized molecules, and therefore, it normally has poor cell attachment.[26–28]

To investigate the attachment of PC12 neuronal cells on the RSF scaffold surfaces, RSF solutions, at different concentrations, were spin coated onto clean cover glasses or silicon wafers. AFM images (Fig. 1A) demonstrated different surface topographies, and consequently cell attachment. The RSF coated glass surfaces (both 5 and 40 mg/mL) showed smooth coated layers (Fig. 1A(a-b)) with roughness's at the nanoscale ( $0.78 \pm 0.02$  nm and  $0.93 \pm 0.01$  nm). The RSF scaffolds investigated here showed poor performance in cell attachment and spreading using PC12 neuronal cells (Fig. 1A(d-e)). A significant decrease in cell density on the surfaces (Fig. 1B) was observed using RSF coated glasses both at 5 mg/mL ( $9600 \pm 700$  cells/cm<sup>2</sup>) and 40 mg/mL ( $900 \pm 600$  cells/cm<sup>2</sup>) as substrates compared to clean glass ( $21900 \pm 1600$  cells/cm<sup>2</sup>), which demonstrates that PC12 cells have a low binding efficiency to RSF coated substrates. These results indicate that RSF coatings, in particular at high concentrations, can be used as cell-repellent surfaces for PC12 cells. When combined with cell adhesive moieties, surfaces could be used to pattern PC12 cells, to guild the growth of the cells.

To enhance cell attachment, composite RSF scaffolds have been widely used to facilitate the cell affinity.[25] RSF scaffolds are normally combined with cell recognized molecules such as collagen, gelatin and PLL to enhance cell attachment. For example, gelatin was cross-linked with RSF scaffolds for the repair of cartilage injury *in vitro* and *in vivo*. [44] The scaffolds not only provided a mechanical protection before neocartilage formation, but also a suitable 3D microenvironment for BMSC (endogenic bone marrow stem cells) proliferation, differentiation, and ECM production. RSF scaffolds have also been modified with RGD sequences through the side groups of aspartic and glutamic acids to improve the cell adhesion.[25] While the previous methods mostly involved chemical modification of the SF material through covalently bonding, here we use the electrostatic interaction of self-assembled cationic peptide nanofibers to enhanced the cell attachment onto the SF scaffolds.

### 3.2. Characterization of RSF/I<sub>3</sub>K scaffolds

The peptide AC-I<sub>3</sub>K-NH<sub>2</sub> (in short I<sub>3</sub>K) was able to self-assemble into long and uniform nanofibers after incubation as previously reported.[37,38] According to previous studies[37], the self-assembly process of I<sub>3</sub>K is a dynamic process via non-covalent interactions. Upon complete dissolution of I<sub>3</sub>K molecules, small I<sub>3</sub>K fragments form interdigitated bilayers with hydrophobic iso-

leucine residues kept in the interior, and charged lysine located on the surface of bilayers. Small I<sub>3</sub>K fragments then assemble into short stacks through hydrophobic interactions and hydrogen bonding. Subsequently, based on molecular chirality and surface curving, these stacks tend to grow into twisted fibres. Further growth of which leads to the formation of long and uniform nanofibers. The width of the formed nanofibers was around 50 nm (Figure S1) while the length of the nanofibers can reach up to 10 μm. Persistence length is a characteristic length scale that has been used to determine the conformation of a uniform chain length.[45] Cox et al.[46] recently measured the contour length (the distance between two ends of I<sub>3</sub>K fibres) by AFM and stochastic reconstruction microscopy and then used this value to calculate persistence length of I<sub>3</sub>K fibres. Their results indicated that self-assembled I<sub>3</sub>K fibres have an average contour length of around 6 μm and persistence length of  $10.1 \pm 1.2$  μm.

AFM was further used to characterise how concentrations of I<sub>3</sub>K affect the surface topography of the I<sub>3</sub>K coated RSF scaffolds. As shown in Fig. 2(a), only a few self-assembled nanofibers were observed on the 1 mg/mL I<sub>3</sub>K coated RSF scaffolds. By increasing the concentration of I<sub>3</sub>K, the number of nanofibers increased gradually forming a near full coverage at 3 mg/mL (Fig. 2(b-c)). Further increasing the concentration of I<sub>3</sub>K resulted in more stacked self-assembled nanofibers, which can potentially lead to cell detachment during cell culture. No significant difference of surface topography between the multi-material RSF/I<sub>3</sub>K scaffold (at concentration ratio 40:5) and I<sub>3</sub>K-only scaffold (5 mg/mL coated glass) could be detected. However, I<sub>3</sub>K-only scaffolds assembled on blank glass could easily be washed off when immersed in the aqueous solutions due to low adhesion properties to the glass surface (Figures S2 and S3), hence making it ineffective for cell culture applications. Therefore, the multi-material combination of I<sub>3</sub>K and RSF generates a structurally stable scaffold that can easily withstand normal cell culture procedures and thus provides an excellent way to generate peptide-based scaffolds for cell culture applications. The strong adhesion between RSF (negatively charged) and I<sub>3</sub>K (positively charged) is a result of the strong electrostatic charge-charge interactions.[37,38]

### 3.3. Neuronal cell attachment and morphology on RSF/I<sub>3</sub>K scaffolds

To investigate PC12 neuronal cell attachment and viability on different RSF/I<sub>3</sub>K scaffold surfaces, a live / dead assay was carried

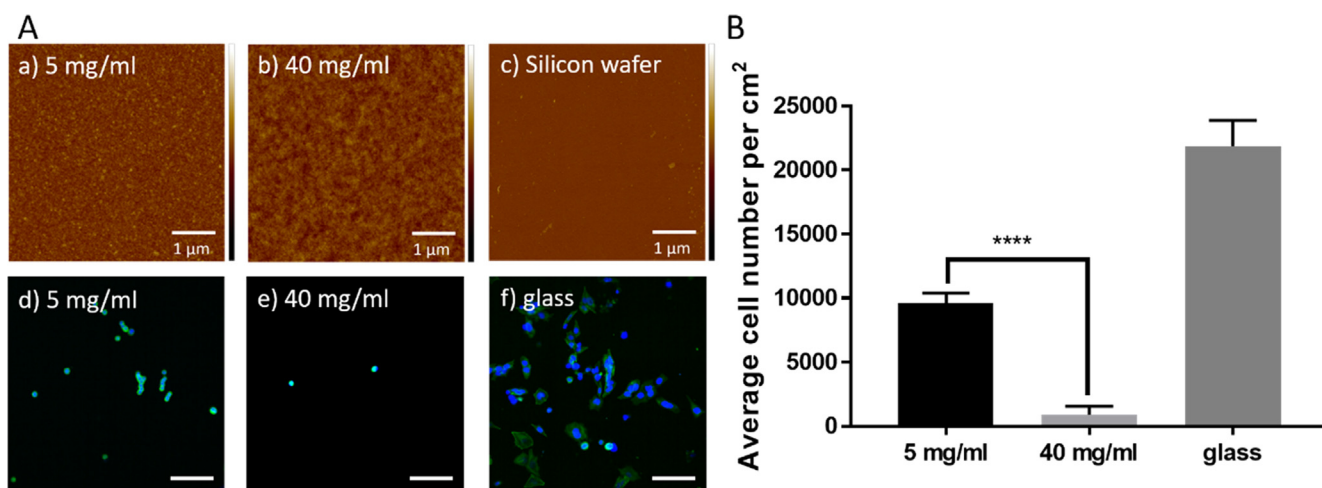


**Fig. 1.** A. AFM topographical images of RSF coated scaffolds on Si-wafers at (a) 5 mg/mL; (b) 40 mg/mL and (c) bare silicon wafer control, Z scale height = 30 nm. Fluorescence images of PC12 cells attached to (d) 5 mg/mL and (e) 40 mg/mL RSF coated surfaces and (f) glass control. (Blue: DAPI staining for nucleus. Green: FITC-phalloidin staining for F-actin.) Scale bar = 100 μm. B. Average cell numbers (per cm<sup>2</sup>) attached to the RSF coated surfaces at RSF concentrations of 0 (glass control), 5 and 40 mg/mL. n ≥ 3, \*\*\*\*p < 0.0001. (For interpretation of the references to colour in this figure legend, the reader is referred to the web version of this article.)

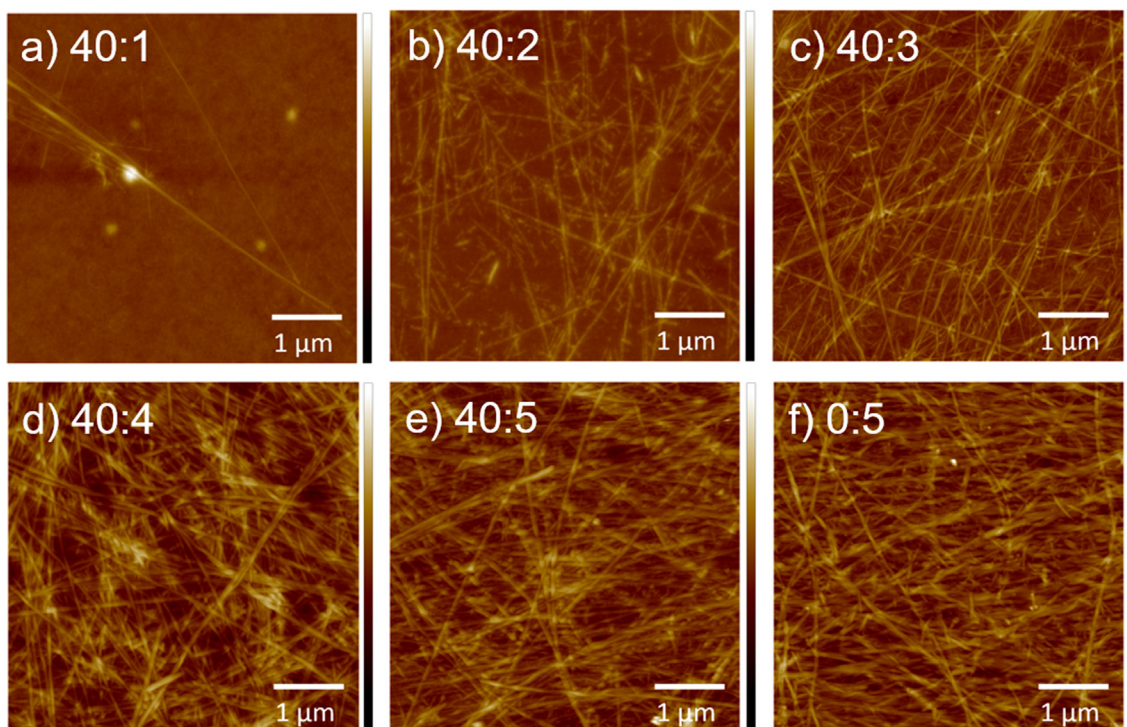


**Fig. 2.** AFM topographical images ( $25 \mu\text{m}^2$ ) showing 1-layer RSF/I<sub>3</sub>K scaffolds coated at different concentration ratios: (a) 40:1, (b) 40:2, (c) 40:3, (d) 40:4, (e) 40:5, (f) 0:5. The Z scale (height) for all images is 120 nm.

out as shown in **Figure S4**. RSF-only scaffolds showed very low cell adhesion due to a lack of cell recognizable groups such as RGD. Furthermore, they are negatively charged, which has been known to have negative effects on cell attachment.[47,48] Therefore, by adding positively charged I<sub>3</sub>K peptide nanofibers onto the negatively charged RSF substrates, the positively charged lysine residues deposited on the scaffold surface promoted PC12 cell binding.[49] PC12 cells showed poor attachment on I<sub>3</sub>K-only and RSF/I<sub>3</sub>K scaffolds at low I<sub>3</sub>K concentrations (<3 mg/mL) compared with RSF/I<sub>3</sub>K scaffolds with high I<sub>3</sub>K concentrations (3–5 mg/mL). This is most likely because I<sub>3</sub>K nanofibers are easily washed off without RSF base during cell culture as shown in the AFM images in **Figures S2 and S3**, and the RSF/I<sub>3</sub>K scaffolds with low concentrations of I<sub>3</sub>K provide insufficient anchoring points for cell attachment. A significant difference in cell density was observed between RSF-only and RSF/I<sub>3</sub>K (3–5 mg/mL) scaffolds, indicating the promotion of PC12 neuronal cell attachment on RSF/I<sub>3</sub>K scaffolds through the addition of positively charged I<sub>3</sub>K nanofibers. However, with an I<sub>3</sub>K concentration of 5 mg/mL, the number of cells decreased slightly, where no cell attachment in some areas was observed. This was possibly due to some detachment of stacked I<sub>3</sub>K nanofibers occurring at this and higher concentrations, as previously discussed in section 3.2. The stacked I<sub>3</sub>K nanofibers promoted excessive cell attachment and cells grew quickly becoming over confluent during the incubation time, thus detaching from the scaffold surface. Additionally, the live / dead assay indicated that RSF/I<sub>3</sub>K scaffolds have excellent biocompatibility. The results indicated that I<sub>3</sub>K is a promising candidate which can be used as a functional scaffold material similar to other peptides (such as PLL[49] or gelatin[4]) previously reported for tissue engineering.

The investigation of cell morphology attached on different ratios of RSF/I<sub>3</sub>K scaffolds was carried out via AFM (**Fig. 3A and S5**). As previously noted, cells spread out well on I<sub>3</sub>K-only coated surfaces but showed patchy attachment due to the peptide being

washed off during cell culture. Cells showed an excellent spreading on I<sub>3</sub>K-only coated surfaces (**Fig. 3A(a)**) whereas cells barely spread out their terminals on RSF-only coated surfaces (**Fig. 3A(b)**). Cells started to attach on RSF/I<sub>3</sub>K coated surfaces at concentration ratio 40:1 (**Fig. 3A(c)**). By increasing the concentration of I<sub>3</sub>K from 2 to 4 mg/mL deposited onto RSF (40 mg/mL) coated surfaces, cellular spreading improved drastically (**Fig. 3A(d-g)**), indicating a peptide concentration dependence of cell spreading. Additionally, FITC-phalloidin and DAPI was used to stain actin filaments and cell nuclei respectively to further characterize the morphology of cells adhered on RSF/I<sub>3</sub>K scaffolds (**Figures S6**). Cells on RSF/I<sub>3</sub>K coated substrates also showed excellent spreading and flattening with this being enhanced as the concentration of coated I<sub>3</sub>K increased. These results are consistent with previous AFM results shown in **Fig. 3A**.

The first step of the cell adhesion process is the cell-polymer interactions, which is essential for cell communication, regulation, tissue development and maintenance.[50,51] Cell-polymer interactions can be divided into three types, i.e. non-adhesion, passive adhesion and active adhesion.[50] The interactions between cells and RSF surfaces corresponds to passive adhesion, which means cells attach easily but can also easily detach from surfaces.[52] Cells attached on RSF/I<sub>3</sub>K scaffolds on the other hand undergo active adhesion, in which cells spontaneously adhere onto the surface and the adhesion is tight, therefore, it is difficult for cells to detach.[53] Additionally, the positively charged lysine residues in I<sub>3</sub>K activates cell changing morphology and causes spreading for attachment-dependent phenotypes. Furthermore, there are three phases that can describe the process of cell adhesion onto cell-active polymer surfaces. Cells adhere onto the RSF-only scaffolds via complex physicochemical interactions including Van-der-Waals, coulombic and hydrophobic forces, known as Phase I cell attachment.[54] The action of the cells starting to spread and become flattened on the RSF/I<sub>3</sub>K scaffold surface (**Fig. 3A(c-d)**), due to integrin binding, is known as Phase II. Full spreading and

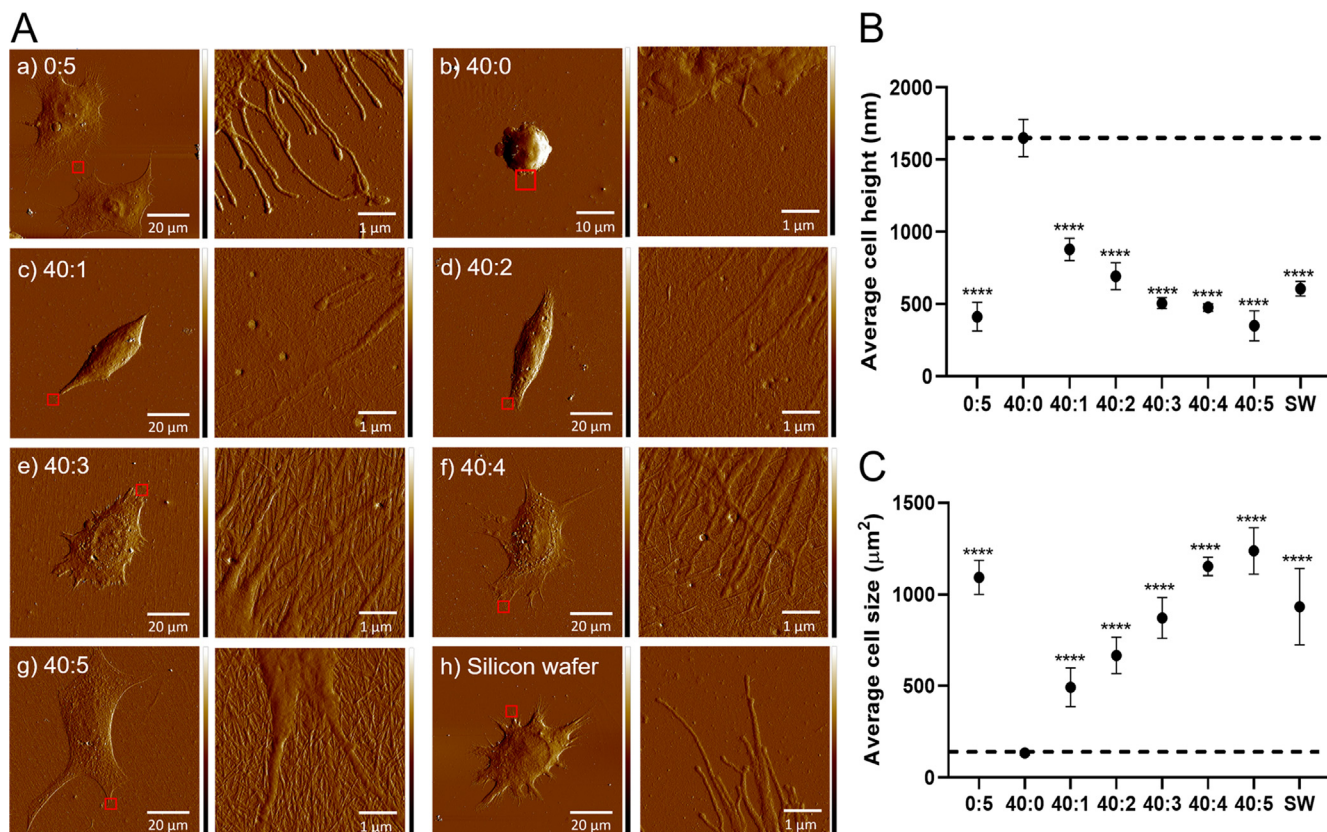


**Fig. 3.** **A**, AFM Peak Force Error images of PC12 neuronal cells attached on a series of RSF and I<sub>3</sub>K coated surfaces. In addition, enlarged AFM images of red box areas are shown in right of each image. The concentration ratios of RSF and I<sub>3</sub>K were: (a) 0:5, (b) 40:0, (c) 40:1, (d) 40:2, (e) 40:3, (f) 40:4, (g) 40:5 and (h) silicon wafer control. The force setpoint constant is 30 nN for images of cells and 5 nN for enlarged areas. **B** and **C** indicate average cell heights and sizes in all scenarios. ( $n \geq 3$ ; \*\*\*\*  $p < 0.0001$ ; \*\*\*  $p < 0.001$ ; and \*  $p < 0.05$ ). (For interpretation of the references to colour in this figure legend, the reader is referred to the web version of this article.)

formation of focal adhesions for the cytoskeleton of PC12 neuronal cells on the RSF/I<sub>3</sub>K (Fig. 3A(e-g)) is regarded as Phase III. Therefore, RSF/I<sub>3</sub>K scaffolds, where I<sub>3</sub>K can be considered a cell-adhesive polymer, are able to activate the cell adhesion process inducing spreading and flattening. Increasing the concentration of I<sub>3</sub>K resulted in improved and expedited cell adhesive properties.

Further AFM analysis revealed the average cell height (Fig. 3B) on RSF-only scaffolds was  $1650 \pm 110$  nm. In the case of I<sub>3</sub>K-only scaffolds, an average cell height of  $410 \pm 80$  nm was measured. The average height of cells on RSF/I<sub>3</sub>K peptide scaffolds decreased with increasing I<sub>3</sub>K concentrations (1 to 5 mg/mL) from  $880 \pm 60$  nm to  $350 \pm 90$  nm. For the blank silicon wafer, the average cell height was  $600 \pm 40$  nm, which was similar to (but slight lower than) that of the RSF/I<sub>3</sub>K (ratio 40:2) samples. The average size of attached cells (Fig. 3C) on RSF-only scaffolds was found to be  $140 \pm 10 \mu\text{m}^2$ . A gradual size increase (up to 9-fold at 5 mg/mL I<sub>3</sub>K) was observed as I<sub>3</sub>K concentration was increased. Both average cell height and size on the silicon wafer substrates were similar to the RSF/I<sub>3</sub>K scaffold at a concentration ratio of 40:3. The results indicated that RSF/I<sub>3</sub>K scaffolds with I<sub>3</sub>K concentrations above 3 mg/mL are ideal for PC12 cell adhesion and spreading, outperforming the cell behaviour on RSF-only scaffolds. The red boxes in Fig. 3A also indicate areas of interest that were enlarged to further investigate the cell morphology. The AFM images show neurites of PC12 cells adhering to the RSF-only or RSF/I<sub>3</sub>K coated surfaces (Fig. 3A(b-g)). In contrast to I<sub>3</sub>K-only scaffolds, Fig. 3A(h) shows the neurites of PC12 cells adhering on exposed bare silicon wafer substrate. The results were similar to those reported by Gupta et al.[55] who indicated that neural cells can adhere and differentiate on chitosan-based scaffolds. We conclude that I<sub>3</sub>K can promote PC12 cell attachment, spreading and neurite formation.

### 3.4. Differences between RSF/I<sub>3</sub>K scaffolds and collagen scaffolds on the function of PC12 cells

Collagen is one of the basic components of the ECM that can provide a natural environment for cell growth, and proliferation, and is widely used in nerve tissue repair.[56,57] In addition, collagen has been proven to possess a good adherence and proliferation ability for PC12 cells.[58] Therefore, the following experiments, including resazurin assay, live / dead assay and immunostaining of neurites, were carried out comparing the differences in PC12 cell functions on RSF/I<sub>3</sub>K scaffolds and collagen scaffolds. Note that, three types of RSF/I<sub>3</sub>K scaffolds were chosen, where the RSF scaffold concentration was 40 mg/mL and RSF/I<sub>3</sub>K scaffold concentration ratios were 40:3 and 40:4 (represented as RSF/I<sub>3</sub>K 40:3 and RSF/I<sub>3</sub>K 40:4).

The metabolic activity of PC12 cells on sample surfaces (Type I collagen; RSF; RSF/I<sub>3</sub>K 40:3 and RSF/I<sub>3</sub>K 40:4) was determined after 24, 72 and 144 h in culture using a resazurin assay, and control groups performed on bare glass and TCP (tissue culture plastic) substrates (Fig. 4). Metabolic activity was observed to increase gradually between 24 and 144 h on all surfaces. Cells adhered on RSF coated surfaces showed the lowest metabolic activity amongst all test surfaces at 24 and 144 h, while for RSF/I<sub>3</sub>K scaffolds, the metabolic activity increased more, indicating I<sub>3</sub>K can promote PC12 cell proliferation. RSF/I<sub>3</sub>K scaffolds at a ratio of 40:4 showed the highest metabolic activity which surpassed that of Type I collagen scaffolds (between 24 and 144 h), indicating a difference in proliferation on the surfaces. For control groups, cells on glass had a lower metabolic activity at all time points in contrast to TCP. The highest cell metabolic activity was observed on TCP samples compared to test surfaces at 24 h. However, the increase in

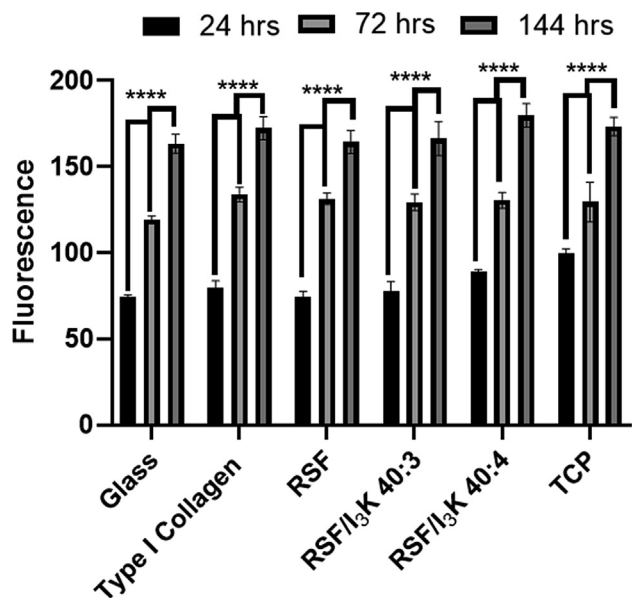


**Fig. 4.** Metabolic activity of PC12 cells adhered on different surfaces assessed using resazurin assay after 24-, 72-, and 144-hours culture. TCP represents tissue culture plastic. (n ≥ 3; \*\*\*\*p < 0.0001).

metabolic activity observed on the TCP surface between 72 and 144 h was similar to that of the other surfaces. This indicates excellent cell proliferation on the coated surfaces.

Live / dead assay results (Fig. 5) indicated a low rate of cell mortality on all surfaces after 6 days of culture. As can be seen from Fig. 5B, there was a slightly lower proportion of live cells on type I collagen (96.7% ± 0.3%) compared to RSF (100%), RSF/I<sub>3</sub>K 40:3 (99.3% ± 0.1%) and RSF/I<sub>3</sub>K 40:4 (98.4% ± 0.2%) scaffolds. Although

collagen is a well-known biocompatible material[59], RSF/I<sub>3</sub>K showed better cell growth and proliferation overall. The population of cells adhered onto uncoated RSF surfaces was poor (Fig. 5C), only 34 ± 28 cells were observed, which is much lower than the adherence onto RSF/I<sub>3</sub>K 40:3 (180 ± 50) and RSF/I<sub>3</sub>K 40:4 (290 ± 50). Please note that, I<sub>3</sub>K coated on RSF surfaces, resulted in a significant difference in observed percentage of live cells. That is due to RSF surfaces having a poor cell attachment, resulting in cells easily detaching from the RSF surfaces during cell culture, and only a few cells remaining. The results demonstrated that I<sub>3</sub>K coated on RSF scaffolds can increase neuronal cell proliferation and attachment. Furthermore, the population of cells increased with increasing I<sub>3</sub>K concentration, which is consistent with the results reported in section 3.3. According to Wiatrak et al.[58], PC12 Adh cells show good attachment on plastic surfaces. As can be seen in Fig. 5C (results obtained from much larger areas than showed in Fig. 5A), there is no significant difference between RSF/I<sub>3</sub>K 40:4 and TCP (note that cells on TCP showed patches with some areas having more cells (e.g., Fig. 5A(f)) and some areas having less). Therefore, RSF/I<sub>3</sub>K 40:4 scaffold also promotes good PC12 cell attachment. However, there was still a significant higher cell population (650 ± 30) on type I collagen than RSF/I<sub>3</sub>K 40:4 scaffolds, indicating that peptides with multiple amino acids / functional groups are required to increase cell densities. The main amino acids in the collagen peptide are glycine, proline and alanine,[59] which can be used as building blocks to further design a modified self-assembled peptide based on I<sub>3</sub>K to improve the performance in nerve tissue engineering.[60]

PC12 neuronal cells were labelled for β III-tubulin, a specific neurite formation marker (Fig. 6A). Short neurite outgrowth was observed for cells adhered to uncoated RSF surfaces and on glass substrates. However, at an I<sub>3</sub>K concentration of 3 mg/mL coated onto RSF surfaces, neurite formations were observed, but slightly shorter than those on cells grown on type I collagen. With increas-

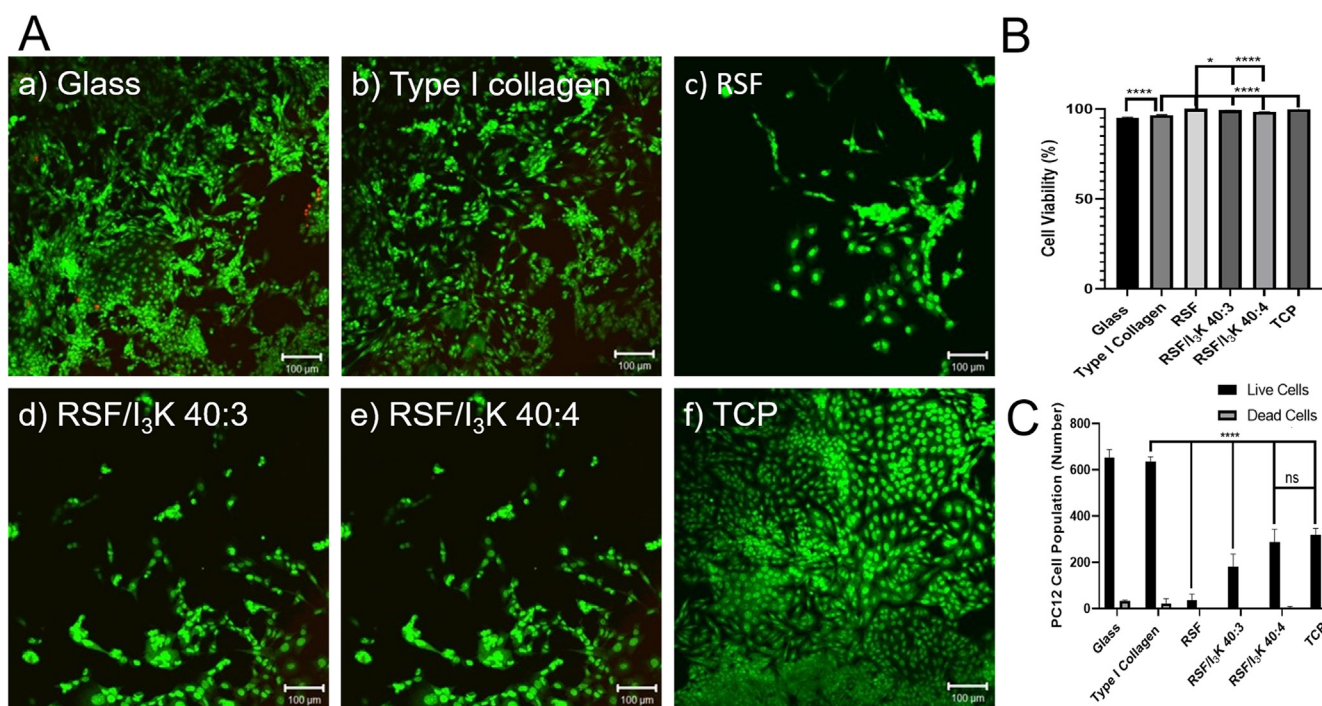


**Fig. 5.** A, Representative confocal images of live / dead analysis from PC12 neuronal cell culture on different surfaces, (a) Glass (control); (b) Type I collagen; (c) RSF; (d) RSF/I<sub>3</sub>K 40:3; (e) RSF/I<sub>3</sub>K 40:4 and (f) TCP (control). The live cells (green) were stained by Syto-9™ and dead cells (red) were stained by propidium iodide, scale bar = 100 μm. B, Percentage of cell viability. C, The population of live and dead cells. TCP represents tissue culture plastic. (n ≥ 3; \*\*\*\*p < 0.0001). (For interpretation of the references to colour in this figure legend, the reader is referred to the web version of this article.)

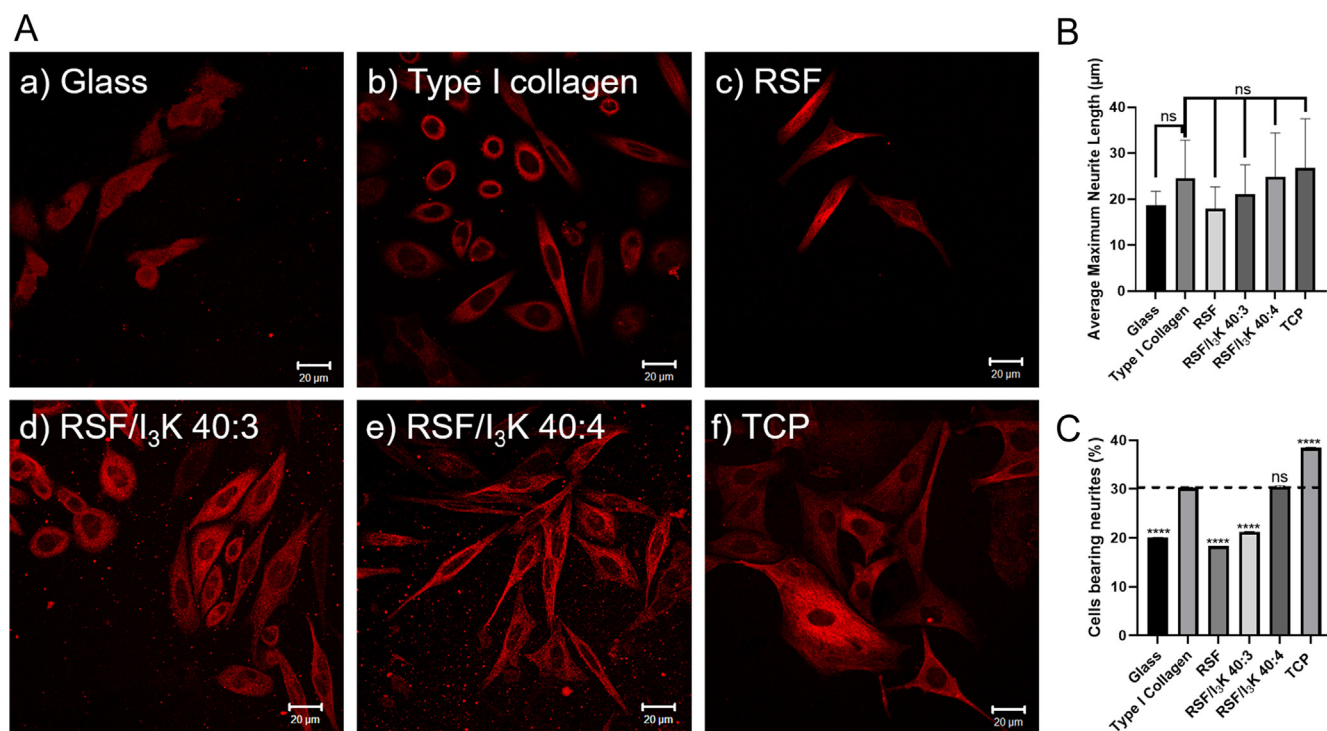


**Fig. 6.** **A**, confocal images of PC12 neuronal cells adhered onto different surfaces, including (a) Glass (control); (b) Type I collagen; (c) RSF; (d) RSF/I<sub>3</sub>K 40:3; (e) RSF/I<sub>3</sub>K 40:4 and (f) TCP (control). Neurites (red) were stained by anti-β III-tubulin, scale bar = 20 μm. **B** and **C** indicate average neurite lengths and the percentage of cells bearing neurites in all scenarios. TCP represents tissue culture plastic. (n ≥ 3; \*\*\*\* p < 0.0001). (For interpretation of the references to colour in this figure legend, the reader is referred to the web version of this article.)

ing concentration of I<sub>3</sub>K to 4 mg/mL, longer neurite formation was observed, which indicated that the concentration of I<sub>3</sub>K directly affects the length of neurites (Fig. 6B), which is consistent with the previous AFM images (Fig. 3). The measurement of average maximum neurite lengths per neuronal cell revealed no significant difference between cells grown on type I collagen (25 ± 8 μm) and RSF/I<sub>3</sub>K 40:4 surfaces (Fig. 6B). Experiments were terminated after 6 days, due to long neurite lengths being physically impaired at high cell density.[61] Comparison to glass and RSF surfaces, type I collagen and RSF/I<sub>3</sub>K 40:4 surfaces had significantly higher percentage of cells bearing neurites (Fig. 6C). However, no significant difference was observed between type I collagen and RSF/I<sub>3</sub>K 40:4 surfaces, suggesting that I<sub>3</sub>K at a concentration of 4 mg/mL possesses similar neuronal cell differentiation to type I collagen.

### 3.5. Micropatterning PC12 cells on RSF scaffolds via inkjet printing of peptide nanofibers

The micro-patterning of complex biomaterial structures plays an essential role in guiding cell adhesion, migration, differentiation and proliferation.[62,63] Inkjet printing can be used as an effective tool to micro-pattern complex structures of biomaterials onto a vast variety of bio-substrates including protein scaffolds[64]. Therefore, it has been deployed here to print I<sub>3</sub>K (3 mg/mL) peptide nanofibers as the letters “SHEF” onto RSF (40 mg/mL) coated substrates. Cell culture studies revealed cells grew almost exclusively along the printed I<sub>3</sub>K letters as shown in Fig. 7. The results were consistent with those reported by Poudel et al.[11] who used photolithography to pattern collagen type I on cell-repellent surfaces and demonstrated neural cell growth along the patterns. It was noticed that PC12 cells prefer to grow on the edge of the letter lines rather than their central areas. This is attributed to the so-called

‘coffee ring effect’ resulting from the inkjet printing process, thus resulting in more I<sub>3</sub>K nanofibers accumulating on the edge of the letters. [65,66] It is possible to reduce this effect by the addition of additives to alter the surface tension and spreading of the I<sub>3</sub>K ink during the printing process, which might be deemed beneficial in the future. In nerve tissue engineering, the alignment of cells is important in axonal regeneration and direction [42]. Therefore, we have shown here the micro-patterning of PC12 cells via inkjet printing of the self-assembled I<sub>3</sub>K peptide nanofibers onto RSF substrates may provide an excellent approach to enable the analysis of axonal development *in vitro*. [64,67]

## 4. Conclusions

The surfactant-like ultrashort peptide I<sub>3</sub>K is able to self-assemble into nanofibrillar structures with a hydrophobic isoleucine tailed fibre core, and positively charged lysine residues located outside the fibres.[46,68] The self-assembled I<sub>3</sub>K peptide nanofibers have been successfully used as templates for the fabrication of silica nanotubes.[37] In this study, I<sub>3</sub>K peptide nanofibers were used as a cell-attractive agent to modify RSF scaffold surfaces to encourage neuronal cell (PC12 cell) attachment and growth. Commonly, positively charged PLL has been used for facilitating cell attachment and proliferation[69,70]. However, PLL can be cytotoxic, especially due to its high-molecular-weight.[71] Therefore, the structure of PLL should be modified via incorporation of segments that can reduce toxicity.[72] In addition, the I<sub>3</sub>K peptide used here, is more cost-effective than PLL due to its short sequence. Overall, we speculate that the positively charged I<sub>3</sub>K peptide nanofibers could be used as an alternative to PLL for cell culture and tissue engineering applications.

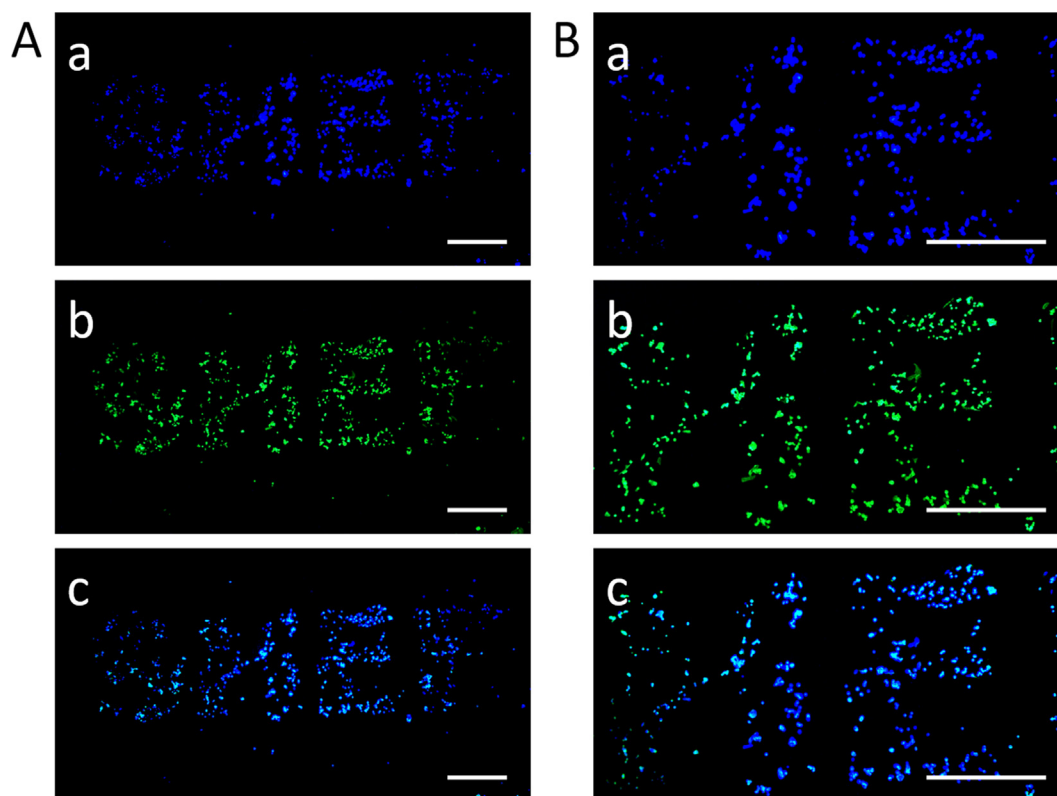


**Fig. 7.** **A,** Inkjet-printing of 1 layer of “SHEF” letters onto RSF coated glass surfaces (40 mg/mL) using I<sub>3</sub>K peptide (3 mg/mL) as the ink, with PC12 neuronal cells growing along the printed letters. **B,** Enlarged letters (“HE”). (a, DAPI staining for nucleus; b, FITC-phalloidin staining for F-actin; c, merged images of a & b), scale bar = 500 μm.

It was found in our study that RSF-only coated surfaces had poor PC12 cell attachment, due to a lack of cell binding functional groups. However, this could be counteracted by introducing I<sub>3</sub>K peptide nanofibers onto the scaffolds during the fabrication process. The peptide nanofibers naturally immobilise onto the RSF scaffold surfaces via charge-charge interactions, where the RSF-only scaffold surface is negatively charged and the I<sub>3</sub>K peptide nanofibers are positively charged. The results showed that the presence of I<sub>3</sub>K peptides promoted PC12 cell binding efficiency as the positively charged lysine residues facilitate cell attachment, which is equivalent to PLL.[39]

Two methods (spin coating and inkjet printing) were applied to prepare scaffolds, with a series of different concentration ratios of RSF and I<sub>3</sub>K onto glass and silicon wafer as substrates. Cells grown on the prepared scaffolds showed variable attachment, proliferation, and morphology including the formation of neurites. Additionally, the live and dead assay demonstrated that both RSF and I<sub>3</sub>K demonstrated negligible cytotoxicity toward PC12 neuronal cells, indicating that both materials are promising scaffold materials for neural tissue engineering. In addition, the RSF/I<sub>3</sub>K (ratio 40:4) produced scaffolds that optimally supported cell adhesion indicating excellent biocompatibility and differentiation. This also demonstrates that the ultra-short peptide I<sub>3</sub>K could be used as an alternative to PLL for cell culture and tissue engineering applications.

Inkjet printing has been shown to be an excellent micro-patterning method for the guidance of cell attachment.[73] The charge-charge interactions between positively charged I<sub>3</sub>K peptide nanofibers and negatively charged RSF coated surfaces facilitated the robustness of the scaffold system during fabrication and cell culture work. Thus, enabling excellent cell growth along the printed patterns. This patterning method is a strength of inkjet printing offering a promising approach for analysing and understanding fundamental cellular functions

such as neurite development and cell–cell interaction *in vitro*. [74,75]

#### CRediT authorship contribution statement

**Weizhen Sun:** Conceptualization, Methodology, Validation, Formal analysis, Investigation, Data curation, Writing - original draft, Visualization. **Caroline S. Taylor:** Methodology, Validation, Formal analysis, Investigation, Data curation, Writing - original draft. **Yi Zhang:** Methodology, Validation, Formal analysis, Investigation, Data curation, Writing - original draft. **David A. Gregory:** Methodology, Writing - review & editing. **Mhd Anas Tomeh:** Writing - review & editing. **John W. Haycock:** Writing - review & editing. **Patrick J. Smith:** Resources. **Feng Wang:** Resources. **Qingyou Xia:** Resources. **Xiubo Zhao:** Conceptualization, Methodology, Writing - review & editing, Visualization, Supervision, Project administration, Funding acquisition.

#### Declaration of Competing Interest

The authors declare that they have no known competing financial interests or personal relationships that could have appeared to influence the work reported in this paper.

#### Acknowledgements

The authors would like to thank the EPSRC (EP/N007174/1 and EP/N023579/1), Royal Society (RG160662 and IE150457) and Jiangsu specially appointed professor program for support.

#### Appendix A. Supplementary material

Supplementary data to this article can be found online at <https://doi.org/10.1016/j.jcis.2021.06.086>.

## References

- [1] Y. Zhu, S.C. Crowley, A.J. Latimer, G.M. Lewis, R. Nash, S. Kucenas, Migratory Neural Crest Cells Phagocytose Dead Cells in the Developing Nervous System, *Cell* 179(1) (2019) 74–89 e10.
- [2] L. Bertram, R.E. Tanzi, The genetic epidemiology of neurodegenerative disease, *J Clin Invest* 115 (6) (2005) 1449–1457.
- [3] D. Singh, A.J. Harding, E. Albadawi, F.M. Boissonade, J.W. Haycock, F. Claeysens, Additive manufactured biodegradable poly(glycerol sebacate methacrylate) nerve guidance conduits, *Acta Biomater* 78 (2018) 48–63.
- [4] R. Boni, A. Ali, A. Shavandi, A.N. Clarkson, Current and novel polymeric biomaterials for neural tissue engineering, *J Biomed Sci* 25 (1) (2018) 90.
- [5] C.E. Schmidt, J.B. Leach, Neural Tissue Engineering: Strategies for Repair and Regeneration, *Annu Rev Biomed Eng* 5 (1) (2003) 293–347.
- [6] J.H.A. Bell, J.W. Haycock, Next Generation Nerve Guides: Materials, Fabrication, Growth Factors, and Cell Delivery, *Tissue Engineering Part B: Reviews* 18 (2) (2012) 116–128.
- [7] X. Gu, F. Ding, D.F. Williams, Neural tissue engineering options for peripheral nerve regeneration, *Biomaterials* 35 (24) (2014) 6143–6156.
- [8] E.A. Huebner, S.M. Strittmatter, Axon regeneration in the peripheral and central nervous systems, *Results Probl Cell Differ* 48 (2009) 339–351.
- [9] A. Bédier, C. Vieu, F. Arnauduc, J.-C. Sol, I. Loubinoux, L. Vaysse, Engineering of adult human neural stem cells differentiation through surface micropatterning, *Biomaterials* 33 (2) (2012) 504–514.
- [10] A. Solanki, S. Shah, K.A. Memoli, S.Y. Park, S. Hong, K.-B. Lee, Controlling Differentiation of Neural Stem Cells Using Extracellular Matrix Protein Patterns, *Small* 6 (22) (2010) 2509–2513.
- [11] I. Poudel, J.S. Lee, L. Tan, J.Y. Lim, Micropatterning–retinoic acid co-control of neuronal cell morphology and neurite outgrowth, *Acta Biomater* 9 (1) (2013) 4592–4598.
- [12] Y. Wu, L. Wang, T. Hu, P.X. Ma, B. Guo, Conductive micropatterned polyurethane films as tissue engineering scaffolds for Schwann cells and PC12 cells, *J Colloid Interface Sci* 518 (2018) 252–262.
- [13] Z. Zhou, S. Zhang, Y. Cao, B. Marelli, X. Xia, T.H. Tao, Engineering the Future of Silk Materials through Advanced Manufacturing, *Adv Mater* (2018) e1706983.
- [14] W. Huang, S. Ling, C. Li, F.G. Omenetto, D.L. Kaplan, Silkworm silk-based materials and devices generated using bio-nanotechnology, *Chem Soc Rev* 47 (17) (2018) 6486–6504.
- [15] G.M. Whitesides, E. Ostuni, S. Takayama, X. Jiang, D.E. Ingber, Soft Lithography in Biology and Biochemistry, *Annu Rev Biomed Eng* 3 (1) (2001) 335–373.
- [16] Y. Xia, G.M. Whitesides, Soft Lithography, *Annu Rev Mater Sci* 28 (1) (1998) 153–184.
- [17] M.K. Gupta, S.K. Khokhar, D.M. Phillips, L.A. Sowards, L.F. Drummy, M.P. Kadakia, R.R. Naik, Patterned Silk Films Cast from Ionic Liquid Solubilized Fibroin as Scaffolds for Cell Growth, *Langmuir* 23 (3) (2007) 1315–1319.
- [18] C. Zhang, Y. Zhang, H. Shao, X. Hu, Hybrid Silk Fibers Dry-Spun from Regenerated Silk Fibroin/Graphene Oxide Aqueous Solutions, *ACS Appl Mater Interfaces* 8 (5) (2016) 3349–3358.
- [19] W. Sun, D.A. Gregory, M.A. Tomeh, X. Zhao, Silk Fibroin as a Functional Biomaterial for Tissue Engineering, *Int J Mol Sci* 22 (3) (2021) 1499.
- [20] M. Floren, C. Migliaresi, A. Motta, Processing Techniques and Applications of Silk Hydrogels in Bioengineering, *J Funct Biomater* 7 (3) (2016) 26.
- [21] W. Zhang, L. Chen, J. Chen, L. Wang, X. Gui, J. Ran, G. Xu, H. Zhao, M. Zeng, J. Ji, L. Qian, J. Zhou, H. Ouyang, X. Zou, Silk Fibroin Biomaterial Shows Safe and Effective Wound Healing in Animal Models and a Randomized Controlled Clinical Trial, *Adv Healthcare Mater* 6 (10) (2017) 1700121.
- [22] L.-P. Yan, J.M. Oliveira, A.L. Oliveira, S.G. Caridade, J.F. Mano, R.L. Reis, Macro/microporous silk fibroin scaffolds with potential for articular cartilage and meniscus tissue engineering applications, *Acta Biomater* 8 (1) (2012) 289–301.
- [23] M. Farokhi, F. Mottaghtalab, Y. Fatahi, A. Khademhosseini, D.L. Kaplan, Overview of Silk Fibroin Use in Wound Dressings, *Trends Biotechnol* 36 (9) (2018) 907–922.
- [24] M. Zhu, K. Wang, J. Mei, C. Li, J. Zhang, W. Zheng, D. An, N. Xiao, Q. Zhao, D. Kong, L. Wang, Fabrication of highly interconnected porous silk fibroin scaffolds for potential use as vascular grafts, *Acta Biomater* 10 (5) (2014) 2014–2023.
- [25] D. Ma, Y. Wang, W. Dai, Silk fibroin-based biomaterials for musculoskeletal tissue engineering, *Mater Sci Eng, C* 89 (2018) 456–469.
- [26] B. Ananthanarayanan, L. Little, D.V. Schaffer, K.E. Healy, M. Tirrell, Neural stem cell adhesion and proliferation on phospholipid bilayers functionalized with RGD peptides, *Biomaterials* 31 (33) (2010) 8706–8715.
- [27] A. Gupta, K.K. Mita, K.P. Arunkumar, J. Nagaraju, Molecular architecture of silk fibroin of Indian golden silkworm *Antheraea assama*, *Sci. Reports* 5 (2015) 12706.
- [28] Y. Qi, H. Wang, K. Wei, Y. Yang, R.-Y. Zheng, I.S. Kim, K.-Q. Zhang, A Review of Structure Construction of Silk Fibroin Biomaterials from Single Structures to Multi-Level Structures, *Int J Mol Sci* 18 (3) (2017) 237.
- [29] A. Leal-Egaña, T. Scheibel, Interactions of cells with silk surfaces, *J Mater Chem* 22 (29) (2012) 14330–14336.
- [30] S. Sofia, M.B. McCarthy, G. Gronowicz, D.L. Kaplan, Functionalized silk-based biomaterials for bone formation, *J Biomed Mater Res* 54 (1) (2001) 139–148.
- [31] S. Aznar-Cervantes, A. Pagán, J.G. Martínez, A. Bernabeu-Esclapez, T.F. Otero, L. Meseguer-Olmo, J.I. Paredes, J.L. Cenis, Electrospun silk fibroin scaffolds coated with reduced graphene promote neurite outgrowth of PC-12 cells under electrical stimulation, *Mater Sci Eng, C* 79 (2017) 315–325.
- [32] D. Lam, H.A. Enright, J. Cadena, S.K.G. Peters, A.P. Sales, J.J. Osburn, D.A. Soscia, K.S. Kulp, E.K. Wheeler, N.O. Fischer, Tissue-specific extracellular matrix accelerates the formation of neural networks and communities in a neuron-glia co-culture on a multi-electrode array, *Sci Rep* 9 (1) (2019) 4159.
- [33] Y.H. Yang, Z. Khan, C. Ma, H.J. Lim, L.A. Smith Callahan, Optimization of adhesive conditions for neural differentiation of murine embryonic stem cells using hydrogels functionalized with continuous Ile-Lys-Val-Ala-Val concentration gradients, *Acta Biomater* 21 (2015) 55–62.
- [34] J.W. Lee, K.Y. Lee, Dual peptide-presenting hydrogels for controlling the phenotype of PC12 cells, *Colloids Surf B Biointerfaces* 152 (2017) 36–41.
- [35] S. Zhang, Fabrication of novel biomaterials through molecular self-assembly, *Nat Biotechnol* 21 (10) (2003) 1171–1178.
- [36] X. Zhao, F. Pan, H. Xu, M. Yaseen, H. Shan, C.A.E. Hauser, S. Zhang, J.R. Lu, Molecular self-assembly and applications of designer peptide amphiphiles, *Chem Soc Rev* 39 (9) (2010) 3480–3498.
- [37] H. Xu, Y. Wang, X. Ge, S. Han, S. Wang, P. Zhou, H. Shan, X. Zhao, J.R. Lu, Twisted Nanotubes Formed from Ultrashort Amphiphilic Peptide 13K and Their Templating for the Fabrication of Silica Nanotubes, *Chem Mater* 22 (18) (2010) 5165–5173.
- [38] Q. Wang, X. Zhang, J. Zheng, D. Liu, Self-assembled peptide nanotubes as potential nanocarriers for drug delivery, *RSC Adv* 4 (48) (2014) 25461–25469.
- [39] J. Wang, L. Tian, N. Chen, S. Ramakrishna, X. Mo, The cellular response of nerve cells on poly-L-lysine coated PLGA-MWCNTs aligned nanofibers under electrical stimulation, *Mater Sci Eng, C* 91 (2018) 715–726.
- [40] H.-Y. Wang, Y.-Q. Zhang, Processing and characterisation of a novel electropolymerized silk fibroin hydrogel membrane, *Sci Rep* 4 (2014) 6182.
- [41] Y.F. Dufreñe, T. Ando, R. Garcia, D. Alsteens, D. Martinez-Martin, A. Engel, C. Gerber, D.J. Müller, Imaging modes of atomic force microscopy for application in molecular and cell biology, *Nat Nanotechnol* 12 (2017) 295.
- [42] Y. Li, G. Huang, X. Zhang, L. Wang, Y. Du, T.J. Lu, F. Xu, Engineering cell alignment in vitro, *Biotechnol Adv* 32 (2) (2014) 347–365.
- [43] G.D. A. Z. Yu, S.P. J. Z. Xiubo, E.S. J. Reactive Inkjet Printing of Biocompatible Enzyme Powered Silk Micro-Rockets, *Small* 12 (30) (2016) 4048–4055.
- [44] W. Shi, M. Sun, X. Hu, B. Ren, J. Cheng, C. Li, X. Duan, X. Fu, J. Zhang, H. Chen, Y. Ao, Structurally and Functionally Optimized Silk-Fibroin-Gelatin Scaffold Using 3D Printing to Repair Cartilage Injury In Vitro and In Vivo, *Adv Mater* 29 (29) (2017).
- [45] S.K. Lakkaraju, W. Hwang, Critical buckling length vs. persistence length: What governs a biofilament conformation?, *Phys. Rev. Letters* 102 (11) (2009) 118102.
- [46] H. Cox, P. Georgiadis, H. Xu, T.A. Waigh, J.R. Lu, Self-Assembly of Mesoscopic Peptide Surfactant Fibrils Investigated by STORM Super-Resolution Fluorescence Microscopy, *Biomacromolecules* 18 (11) (2017) 3481–3491.
- [47] M.M. Jacobsen, D. Li, N. Gyune Rim, D. Backman, M.L. Smith, J.Y. Wong, Silk-fibronectin protein alloy fibres support cell adhesion and viability as a high strength, matrix fibre analogue, *Sci Rep* 7 (2017) 45653.
- [48] B. Panilaitis, G.H. Altman, J. Chen, H.-J. Jin, V. Karageorgiou, D.L. Kaplan, Macrophage responses to silk, *Biomater.* 24 (18) (2003) 3079–3085.
- [49] Y.H. Kim, N.S. Baek, Y.H. Han, M.-A. Chung, S.-D. Jung, Enhancement of neuronal cell adhesion by covalent binding of poly-D-lysine, *J Neurosci Methods* 202 (1) (2011) 38–44.
- [50] L. Chen, C. Yan, Z. Zheng, Functional polymer surfaces for controlling cell behaviors, *Mater Today* 21 (1) (2018) 38–59.
- [51] A.A. Khalili, M.R. Ahmad, A Review of Cell Adhesion Studies for Biomedical and Biological Applications, *Int J Mol Sci* 16 (8) (2015) 18149–18184.
- [52] E. Ito, K. Suzuki, M. Yamato, M. Yokoyama, Y. Sakurai, T. Okano, Active platelet movements on hydrophobic/hydrophilic microdomain-structured surfaces, *J Biomed Mater Res* 42 (1) (1998) 148–155.
- [53] A. Kikuchi, T. Okano, Nanostructured designs of biomedical materials: applications of cell sheet engineering to functional regenerative tissues and organs, *J Control Release* 101 (1) (2005) 69–84.
- [54] T. Okano, N. Yamada, M. Okuhara, H. Sakai, Y. Sakurai, Mechanism of cell detachment from temperature-modulated, hydrophilic-hydrophobic polymer surfaces, *Biomaterials* 16 (4) (1995) 297–303.
- [55] P. Gupta, A. Agrawal, K. Murali, R. Varshney, S. Beniwal, S. Manhas, P. Roy, D. Lahiri, Differential neural cell adhesion and neurite outgrowth on carbon nanotube and graphene reinforced polymeric scaffolds, *Mater Sci Eng, C* 97 (2019) 539–551.
- [56] L. Sbricoli, R. Guazzo, M. Annunziata, L. Gobatto, E. Bressan, L. Nistri, Selection of Collagen Membranes for Bone Regeneration, *Literat. Rev. Mater. (Basel)* 13 (3) (2020).
- [57] X. Lü, H. Zhang, Y. Huang, Y. Zhang, A proteomics study to explore the role of adsorbed serum proteins for PC12 cell adhesion and growth on chitosan and collagen/chitosan surfaces, *Regener Biomater* 5 (5) (2018) 261–273.
- [58] B. Wiatrak, A. Kubis-Kubiak, A. Piwowar, E. Barg, PC12 Cell Line: Cell Types, Coating of Culture Vessels, Differentiation and Other Culture Conditions, *Cells* 9 (4) (2020).
- [59] C. Dong, Y. Lv, Application of Collagen Scaffold in Tissue Engineering: Recent Advances and New Perspectives, *Polymers (Basel)* 8(2) (2016)
- [60] J. Li, J. Wang, Y. Zhao, P. Zhou, J. Carter, Z. Li, T.A. Waigh, J.R. Lu, H. Xu, Surfactant-like peptides: From molecular design to controllable self-assembly with applications, *Coord Chem Rev* 421 (2020) 213418.
- [61] C.J. Pateman, A.J. Harding, A. Glen, C.S. Taylor, C.R. Christman, P.P. Robinson, S. Rimmer, F.M. Boissonade, F. Claeysens, J.W. Haycock, Nerve guides manufactured from photocurable polymers to aid peripheral nerve repair, *Biomater.* 49 (2015) 77–89.

- [62] X. Du, Y. Wang, L. Yuan, Y. Weng, G. Chen, Z. Hu, Guiding the behaviors of human umbilical vein endothelial cells with patterned silk fibroin films, *Colloids Surf, B* 122 (2014) 79–84.
- [63] X. Li, R. You, Z. Luo, G. Chen, M. Li, Silk fibroin scaffolds with a micro-/nanofibrous architecture for dermal regeneration, *J Mater Chem B* 4 (17) (2016) 2903–2912.
- [64] J. Guo, S. Ling, W. Li, Y. Chen, C. Li, F.G. Omenetto, D.L. Kaplan, Coding Cell Micropatterns Through Peptide Inkjet Printing for Arbitrary Biomineralized Architectures, *Adv Funct Mater* 28 (19) (2018) 1800228.
- [65] P. He, B. Derby, Controlling Coffee Ring Formation during Drying of Inkjet Printed 2D Inks, *Adv Mater Interfaces* 4 (22) (2017) 1700944.
- [66] D. Soltman, V. Subramanian, Inkjet-Printed Line Morphologies and Temperature Control of the Coffee Ring Effect, *Langmuir* 24 (5) (2008) 2224–2231.
- [67] K. Kawaguchi, R. Kageyama, M. Sano, Topological defects control collective dynamics in neural progenitor cell cultures, *Nature* 545 (2017) 327.
- [68] S. Han, S. Cao, Y. Wang, J. Wang, D. Xia, H. Xu, X. Zhao, J.R. Lu, Self-assembly of short peptide amphiphiles: the cooperative effect of hydrophobic interaction and hydrogen bonding, *Chemistry* 17 (46) (2011) 13095–13102.
- [69] S. Zheng, Y. Guan, H. Yu, G. Huang, C. Zheng, Poly-L-lysine-coated PLGA/poly (amino acid)-modified hydroxyapatite porous scaffolds as efficient tissue engineering scaffolds for cell adhesion, proliferation, and differentiation, *New J Chem* 43 (25) (2019) 9989–10002.
- [70] M. Kouhi, M. Fathi, M.P. Prabhakaran, M. Shamanian, S. Ramakrishna, Poly L lysine-modified PHBV based nanofibrous scaffolds for bone cell mineralization and osteogenic differentiation, *Appl Surf Sci* 457 (2018) 616–625.
- [71] A. Hall, L.-P. Wu, L. Parhamifar, S.M. Moghimi, Differential modulation of cellular bioenergetics by poly(L-lysine)s of different molecular weights, *Biomacromolecules* 16 (7) (2015) 2119–2126.
- [72] M. Zheng, M. Pan, W. Zhang, H. Lin, S. Wu, C. Lu, S. Tang, D. Liu, J. Cai, Poly( $\alpha$ -L-lysine)-based nanomaterials for versatile biomedical applications: Current advances and perspectives, *Bioact Mater* 6 (7) (2021) 1878–1909.
- [73] P. Rider, Y. Zhang, C. Tse, Y. Zhang, D. Jayawardane, J. Stringer, J. Callaghan, I.M. Brook, C.A. Miller, X. Zhao, P.J. Smith, Biocompatible silk fibroin scaffold prepared by reactive inkjet printing, *J Mater Sci* 51 (18) (2016) 8625–8630.
- [74] C.J. Lee, P. Huie, T. Leng, M.C. Peterman, M.F. Marmor, M.S. Blumenkranz, S.F. Bent, H.A. Fishman, Microcontact Printing on Human Tissue for Retinal Cell Transplantation, *JAMA Ophthalmology* 120 (12) (2002) 1714–1718.
- [75] R. Singhvi, A. Kumar, G. Lopez, G. Stephanopoulos, D. Wang, G. Whitesides, D. Ingber, Engineering cell shape and function, *Science* 264 (5159) (1994) 696–698.